A unified theory of high-harmonic generation: Application to polarization properties of the harmonics

W. Becker,* A. Lohr, and M. Kleber
Physik-Department T30, Technische Universität München, D-85747 Garching, Germany

M. Lewenstein
Commissariat à l'Energie Atomique, DSM/DRECAM/SPAM, Centre d'Etudes de Saclay, F-91191 Gif-sur-Yvette, France
(Received 9 December 1996)

A general framework is given of how to derive expressions for high-harmonic generation in close analogy to the derivation of the Keldysh amplitude for ionization. As in the former, the approximation made consists of neglecting the effect of the binding potential in intermediate states. The approach can be used for arbitrary binding potentials, but is best suited to short-range potentials at high intensities. It is almost exact for a zero-range potential for arbitrary intensity. Various models that have been used before by some of the authors, such as the effective dipole model and the zero-range potential model, emerge as special cases. The relation between the S-matrix element for high-harmonic generation and the dipole-moment expectation value is discussed, as well as the relation of both to the dipole-dipole correlation function. An exact functional relationship between high-harmonic generation and the total ionization rate is presented. For the case of an elliptically polarized monochromatic driving field, the polarization properties of the emitted harmonics, viz. their ellipticity and the offset angle of their polarization ellipse, are evaluated for both the zero-range potential model and the effective-dipole model, and compared. The predictions of both models generally agree, there are, however, some qualitative differences for the harmonics around the end of the plateau.
[S1050-2947(97)05806-X]

PACS number(s): 32.80.Rm, 42.65.Ky

I. INTRODUCTION

The generation of high harmonics of a laser irradiating an ensemble of atoms has turned into a topic of great current interest, both from fundamental and applications-oriented points of view; for a fairly recent review, see Ref. [1]. There are two sides to the underlying physics: each individual atom emits radiation at harmonics of the laser frequency, and all of these wave trains propagate in the environment consisting of the remaining atoms and the ions and electrons set free in the competing process of ionization; they interfere and scatter and may stimulate further harmonic emission. The observed spectrum of harmonics is affected by both the single-atom emission and this ensuing collective behavior and, depending on the situation, one or the other side dominates the experimental results. However, obviously the collective behavior does not produce harmonics if the single atoms do not. In this paper we will concentrate on the harmonic emission of a single atom. In order to realize the complexity of this first step already, one should look at it from the point of view of nonlinear optics. High-harmonic emission, as other phenomena characteristic of intense-laser atom interactions, is highly nonlinear with respect to the atom-field interaction, to the point that perturbation theory of any reasonable finite order becomes inapplicable. Hence one has, in principle, to deal with the entire set of $\chi^{(2n+1)}$ for all n for a many-electron system when just the properties and implications of the lowest order $\chi^{(3)}$ have already opened up a whole new chapter of physics. Fortunately, it has turned out that a ''single-active-electron approximation'' is normally sufficient [2], but this still leaves a formidable problem. Numerical solutions [3] of the time-dependent one-particle Schrödinger equation have contributed significantly to the elucidation of the observed patterns. However, even with today's computing facilities, this meets problems which become insurmountable when it comes to, e.g., the calculation of extremely high harmonics of very low intensity and/or in a truly three-dimensional situation. This is particularly detrimental if one recalls that single-atom behavior is to provide the input for the investigation of the collective aspects that ought to follow.

Because of these considerations, simplified modeling of the single-atom emission has become popular. Various models have reproduced many aspects of the observations, but two such models have turned out to incorporate most of the relevant physics such that they can provide a sufficiently dependable input for the collective side: both simplify the atom down to its absolute essentials. One approximates the atomic binding potential by a zero-range potential [4,5], while the other introduces a model Hamiltonian with just one bound state and an undistorted continuum [6,7]. This latter model leaves some freedom as to the form of the dipole matrix element between the ground state and the continuum. Both models do not account for the effects of excited bound states nor the effect of the binding potential on the electronic motion in the continuum. Moreover, both models, in their simplest versions, ignore depletion of the initial atomic

*Present address: Max-Born-Institut für Nichtlineare Optik und Kurzzeitspektroskopie, 12474 Berlin, Germany. Also at Center for Advanced Studies, Department of Physics and Astronomy, University of New Mexico, Albuquerque, NM 87131.

ground state [8]. This is mended in more refined versions [9–12]. They both lead to comparably manageable integral expressions for the harmonic intensities which can be computed efficiently enough to allow for the subsequent investigation of the collective behavior. Owing to the largely identical assumptions made, it is not surprising that both models produce closely related answers even though the formal expressions look rather different. An additional benefit of these models is that they have given an *a priori* justification for the very intuitive and successful (but less quantitative) semiclassical concepts where the electron returning to its parent ion produces harmonics via recombination [13,14].

In this paper, we will evaluate harmonic generation in strict parallelism to the Keldysh-Faisal-Reiss [15] framework for ionization. In fact, one crucial approximation necessary for ionization is not required for harmonic generation. This is the approximation of the final (field-free) scattering state of the electron by a plane wave. We will discuss how both of the aforementioned models fit into this more general context. In general, the predictions of the two models come out to be very close. For a particularly sensitive comparison, we investigate the polarization properties of the harmonics near the cutoff for an elliptically polarized driving field. In this case, some characteristic discrepancies do show up.

In Sec. II, we start with a reminder of the derivation of the Keldysh amplitude, tailored to our particular needs. Next, we try to follow precisely the same steps in the evaluation of the ground-state expectation value of the atomic dipole moment, the key ingredient for the computation of the harmonic spectrum. One of the terms that contributes to the dipole moment can be identified as a continuum-continuum interaction. If this term is disregarded, the effective-dipole model of Lewenstein and co-workers [6,7] is recovered. If, on the other hand, the term is kept, the entire dipole moment can be rewritten in the form of one single term which has exactly the form of the continuum-continuum term, except that the explicitly showing interactions with the external field are replaced by the binding potential. If the latter is replaced by a zero-range potential, then the dipole moment reduces to the expressions employed earlier for this case [4,5]. For a general potential, the entire expression for the dipole moment can also be rewritten in a form whose structure is close to that of the effective-dipole model [6,7], but containing one additional integration over time which is related to the emission of the harmonic photon. In Sec. II D, we adopt a different starting point by calculating the *S-matrix element* for harmonic emission of *exactly one photon* rather than the dipole moment expectation value. For low harmonic efficiencies—in fact throughout the entire spectrum with the exception of the very lowest harmonics—the two approaches yield virtually identical numerical results. However, the formal structure of the S-matrix element is more appealing, and lends itself immediately to an interpretation in terms of classical orbits departing from and returning to the position of the ion. In Sec. II E, we derive an exact general relation between ionization and harmonic generation. We show that the latter can be computed via the functional derivative of the ground-state persistence amplitude with respect to the driving external field. This relation holds only for the S-matrix element, and not for the dipole expectation value.

In Sec. III, we concentrate on polarization properties of the emitted harmonics for an elliptically polarized driving field, that is, on the ellipticities of the harmonics and the offset angle of their polarization ellipse with respect to that of the driving field. We consider harmonics both in the lower part of the plateau and near the cutoff. Generally, in the lower part of the plateau, the polarization characteristics do not exhibit distinctive qualitative features, but they do so near the cutoff. It is also in this region that we find discrepancies between the zero-range potential model [4,5] and the effective-dipole model [6,7]. Whether or not some of these qualitative effects will survive as such after propagation through the medium remains an open question.

In Sec. IV, we summarize our conclusions. Finally, we use the Appendix to discuss the relation of both the dipole moment expectation value and the S-matrix element to the dipole-dipole correlation function, which is known to specify the total number of emitted photons.

II. FORMAL DEVELOPMENTS

A. Ionization amplitude

Let us first recall the assumptions and approximations made in the derivation of the Keldysh ionization amplitude. The transition amplitude from the ground state before the arrival of the laser pulse to the final state after the pulse has passed is

$$M_{\mathbf{p}}=\lim_{t\to\infty}\langle\psi_{\mathbf{p}}(t)|\Psi(t)\rangle. \tag{2.1}$$

Here $\Psi(t)$ denotes the exact wave function that has developed out of the initial ground state, while $\psi_{\mathbf{p}}$ is a scattering state with asymptotic momentum $\mathbf{p}$ in the presence of the atomic binding potential, but in the absence of the laser field. We may use the full time-evolution operator U, taking into account both the binding potential and the laser field in order to propagate the exact wave function from time t backwards to some time before the arrival of the pulse, so that

$$\begin{aligned}M_{\mathbf{p}}&=\lim_{t\to\infty,t'\to-\infty}\langle\psi_{\mathbf{p}}(t)|U(t,t')|\Psi(t')\rangle\\&=\lim_{t\to\infty,t'\to-\infty}\langle\psi_{\mathbf{p}}(t)|U(t,t')|\psi_0(t')\rangle.\end{aligned} \tag{2.2}$$

In the last line of Eq. (2.2), we used the fact that in the limit of early times, $t'\to-\infty$, the exact wave function $\Psi(t)$ reduces to the unperturbed (field-free) wave function $\psi_0(t)$ of the initial ground state. Next, we will make use of the Dyson equation for the time-evolution operator,

$$\begin{aligned}U(t,t')&=U_0(t,t')-i\int_{t'}^{t}dt''U_0(t,t'')H_I(t'')U(t'',t')\\&=U_0(t,t')-i\int_{t'}^{t}dt''U(t,t'')H_I(t'')U_0(t'',t').\end{aligned} \tag{2.3}$$

Here U_0 is the time-evolution operator in the presence of merely the binding potential and $H_I(\mathbf{r}t)=-e\mathbf{r}\cdot\mathbf{E}(t)$ the interaction with the laser field. The atomic propagator $U_0(t,t')$ propagates the field-free atomic-ground-state wave

function $\psi_0(t')$ forward to the finite time t (where, in general, the laser is on). Both U and U_0 are unitary and satisfy the group property

$$U(t,t'')=U(t,t')U(t',t''). \tag{2.4}$$

Moreover, as a consequence of unitarity, the initial condition $U(t,t)=1$, and the group property, we have

$$U(t,t')^{\dagger}=U(t',t). \tag{2.5}$$

If we insert the Dyson equation (2.3) in the matrix element (2.2) then, owing to the orthogonality of the initial ground state $|\psi_0\rangle$ and the scattering state $|\psi_{\mathbf{p}}\rangle$, the first term (the one involving just U_0) vanishes. The remaining term can be rewritten in the form

$$M_{\mathbf{p}}=-i\lim_{t\to\infty}\int_{-\infty}^{t}dt'\langle\psi_{\mathbf{p}}(t)|U(t,t')H_I(t')|\psi_0(t')\rangle. \tag{2.6}$$

No approximations have been made up to this point. Notice that the complete time-evolution operator $U(t,t')$ in the amplitude (2.6) accomplishes three things which cannot be strictly separated: It dresses the initial and final states, and it propagates the electron from the former to the latter which includes the possibility of major excursions of its orbit away from the ion. We now make the approximation that is typical of Keldysh theories. We replace the complete time-evolution operator U by the Volkov time-evolution operator $U^{(V)}$, which satisfies

$$i\frac{\partial}{\partial t}U^{(V)}(t,t')=\left(\frac{\hat{\mathbf{p}}^2}{2m}+H_I(t)\right)U^{(V)}(t,t'),$$

$$-i\frac{\partial}{\partial t'}U^{(V)}(t,t')=U^{(V)}(t,t')\left(\frac{\hat{\mathbf{p}}^2}{2m}+H_I(t')\right). \tag{2.7}$$

That is, we neglect the binding potential everywhere except in the initial and final states. As a consequence, the initial and final state are no longer dressed and the electron no longer ''feels'' the binding potential during the propagation. Equation (2.6) now reads

$$\widetilde{M}_{\mathbf{p}}^{(K)}=-i\lim_{t\to\infty}\int_{-\infty}^{t}dt'\langle\psi_{\mathbf{p}}(t)|U^{(V)}(t,t')H_I(t')|\psi_0(t')\rangle. \tag{2.8}$$

An equivalent and often more useful form can be obtained as follows. We rewrite Eq. (2.8) in the form

$$\widetilde{M}_{\mathbf{p}}^{(K)}=-i\lim_{t\to\infty}\int_{-\infty}^{t}dt'\langle\psi_{\mathbf{p}}(t)|U^{(V)}(t,t')\left\{\left[H_I(t')+\frac{\hat{\mathbf{p}}^2}{2m}\right]-\left[\frac{\hat{\mathbf{p}}^2}{2m}+V\right]+V\right\}|\psi_0(t')\rangle, \tag{2.9}$$

where V denotes the atomic binding potential. Owing to Eq. (2.7), the first term in brackets yields $-i(\partial/\partial t')$, acting to the left on the Volkov propagator. An integration by parts with respect to t' then cancels the second term in brackets in Eq. (2.9). Because of the orthogonality of the initial state and the final scattering state the boundary term that occurs in this integration by parts makes no contribution, and the result is just like Eq. (2.8), but with the interaction H_I replaced by the binding potential V,

$$\widetilde{M}_{\mathbf{p}}^{(K)}=-i\lim_{t\to\infty}\int_{-\infty}^{t}dt'\langle\psi_{\mathbf{p}}(t)|U^{(V)}(t,t')V|\psi_0(t')\rangle. \tag{2.10}$$

The limit of $t\to\infty$ is akward to perform. Hence the Keldysh approach makes the additional approximation of replacing the scattering state $\psi_{\mathbf{p}}$ by the plane wave $(2\pi)^{-3/2}\exp[i(\mathbf{p}\cdot\mathbf{r}-Et)]$ which, however, destroys the orthogonality of the initial and final states. This way the Volkov state $\langle\psi_{\mathbf{p}}^{(V)}(t)|$ appears, and we end up with the Keldysh amplitude

$$M_{\mathbf{p}}^{(K)}=-i\int_{-\infty}^{\infty}dt\langle\psi_{\mathbf{p}}^{(V)}(t)|H_I(t)|\psi_0(t)\rangle, \tag{2.11}$$

or with the equivalent form [16,17]

$$M_{\mathbf{p}}^{(K)}=-i\int_{-\infty}^{\infty}dt\langle\psi_{\mathbf{p}}^{(V)}(t)|V|\psi_0(t)\rangle, \tag{2.12}$$

which derives from Eq. (2.10).

It is notoriously difficult precisely to specify the range of validity of the Keldysh amplitudes. Generally speaking, the approximation of replacing the exact propagator $U(t,t')$ by the Volkov propagator $U^{(V)}(t,t')$ works the better the shorter the range of the binding potential and the higher the intensity. Also, circular polarization is more favorable than linear polarization. The aforementioned field-induced energy shift of the initial bound state which is dropped by the approximation could be reintroduced by hand, if desired. The consequences of the additional approximation of replacing the scattering state by a plane wave can be very tricky. For example, for one-photon ionization this approximation has been shown to introduce a spurious gauge dependence [18]. On the other hand, for a zero-range potential (where the scattering state differs from a plane wave only by an s-wave term) and for circular polarization the Keldysh amplitude yields the quasienergy virtually exactly [17].

B. Dipole-moment expectation value

In complete analogy to the preceding derivation of the Keldysh amplitude, we will now derive an approximate expression for the ground-state expectation value

$$\mathbf{R}(t)=\langle\Psi(t)|\mathbf{r}|\Psi(t)\rangle \tag{2.13}$$

of the dipole moment. The approach we will follow has much in common with Ref. [19], but is best suited to intensities that are high (ponderomotive energy exceeding the binding energy) but below the over-the-barrier regime. Again, we use the full propagator in order to relate the field-dressed ground state to the field-free ground state,

$$\mathbf{R}(t)=\lim_{t',t''\to-\infty}\langle\psi_0(t')|U(t',t)\mathbf{r}U(t,t'')|\psi_0(t'')\rangle. \tag{2.14}$$

As above, we apply the Dyson equation (2.3). This yields four terms:

$$\begin{aligned}\mathbf{R}(t)=&\langle\psi_0(t)|\mathbf{r}|\psi_0(t)\rangle\\&-i\int_{-\infty}^{t}dt'\langle\psi_0(t)|\mathbf{r}U(t,t')H_I(t')|\psi_0(t')\rangle\\&+i\int_{-\infty}^{t}dt'\langle\psi_0(t')|H_I(t')U(t',t)\mathbf{r}|\psi_0(t)\rangle\\&+\int_{-\infty}^{t}dt'dt''\langle\psi_0(t')|H_I(t')U(t',t)\mathbf{r}U(t,t'')\\&\times H_I(t'')|\psi_0(t'')\rangle.\end{aligned} \tag{2.15}$$

Here the first term is zero for any spherically symmetric potential. One recognizes that these four terms are such that in terms of Feynman diagrams the vertex for the emission of the harmonic photon (given by $\mathbf{r}$) is inserted in all possible ways. In analogy to the above derivation of the Keldysh amplitude, we now replace the full time-evolution operator U by the Volkov time-evolution operator $U^{(V)}$. In the last three terms of Eq. (2.15), we attempt the same manipulations that led from Eq. (2.8) to Eq. (2.10). In the partial integrations, the boundary terms at $t\to-\infty$ make no contribution, this time owing to the dispersion-related factor of $(t-t')^{-3/2}$ in the time-evolution operator $U^{(V)}(t,t')$. However, boundary terms now survive from $t'=t$ and/or $t''=t$. These terms cause extensive cancellations, and in the end the only term left is

$$\begin{aligned}\mathbf{R}^{(K)}(t)=&\int_{-\infty}^{t}dt'dt''\langle\psi_0(t')|VU^{(V)}(t',t)\mathbf{r}\\&\times U^{(V)}(t,t'')V|\psi_0(t'')\rangle.\end{aligned} \tag{2.16}$$

This is the Keldysh approximation to the dipole moment expectation value. The only approximation made consisted in neglecting the binding potential in the time-evolution operators U in Eq. (2.15). Since only the atomic ground state is involved, the additional approximation of replacing the exact scattering state by a plane wave was not required.

Equation (2.16) can be further simplified. It can be shown [20] that

$$\begin{aligned}&\langle\mathbf{r}'|U^{(V)}(t',t)\mathbf{r}U^{(V)}(t,t'')|\mathbf{r}''\rangle\\&\quad=\mathbf{r}_{\rm class}(t;\mathbf{r}'t',\mathbf{r}''t'')U^{(V)}(\mathbf{r}'t',\mathbf{r}''t''),\end{aligned} \tag{2.17}$$

where

$$\begin{aligned}\mathbf{r}_{\rm class}(t;\mathbf{r}'t',\mathbf{r}''t'')=\frac{1}{t'-t''}\Big\{&(t-t'')\Big(\mathbf{r}'-\frac{e}{m}\int_{t'}^{t}d\tau\,\mathbf{A}(\tau)\Big)\\&-(t-t')\Big(\mathbf{r}''-\frac{e}{m}\int_{t''}^{t}d\tau\,\mathbf{A}(\tau)\Big)\Big\}\end{aligned} \tag{2.18}$$

is the classical orbit of an electron that starts from position $\mathbf{r}''$ at time t'' to the new position $\mathbf{r}'$ at time t' in the presence of the electromagnetic field $\mathbf{A}(t)$. Notice that in view of Eq. (2.16) the initial and final positions $\mathbf{r}''$ and $\mathbf{r}'$ are restricted to within the range of the binding potential $V(\mathbf{r})$.

For the zero-range potential

$$V(\mathbf{r})=\frac{2\pi}{m\kappa}\delta(\mathbf{r})\frac{\partial}{\partial r}r, \tag{2.19}$$

Eq. (2.16) *exactly* reproduces the dipole moment used by some of us in earlier work [4,5]. Actually, for the zero-range potential the expression (2.16) is fairly close to the exact result. This is realized more easily from the earlier derivations [5].

On the other hand, if the fourth term in Eq. (2.15) is dropped, and again the exact time-evolution operator is replaced by its Volkov approximation, we recover the dipole moment employed by Lewenstein and co-workers [6,7]. To see this, we just have to insert the expansion of $U^{(V)}$ in terms of the Volkov wave functions. This yields

$$\begin{aligned}\mathbf{R}^{(L)}=ie\int_{-\infty}^{t}dt'e^{-i|E_0|(t-t')}\int d^3p\,\exp[-iS(\mathbf{p},t,t')]\\\times\mathbf{d}[\mathbf{p}-e\mathbf{A}(t)]^{*}\mathbf{d}[\mathbf{p}-e\mathbf{A}(t')]\cdot\mathbf{E}(t')+\text{c.c.}\end{aligned} \tag{2.20}$$

with

$$S(\mathbf{p},t,t')=\frac{1}{2m}\int_{t'}^{t}d\tau[\mathbf{p}-e\mathbf{A}(\tau)]^2, \tag{2.21}$$

and the dipole transition matrix element

$$\mathbf{d}(\mathbf{p})=(2\pi)^{-3/2}\int d^3\mathbf{r}\,e^{-i\mathbf{p}\cdot\mathbf{r}}\mathbf{r}\psi_0(\mathbf{r})\equiv\langle\mathbf{p}|\mathbf{r}|0\rangle. \tag{2.22}$$

In $\mathbf{R}^{(L)}$, the binding potential does not enter explicitly, but only via the ground-state wave function in the matrix element (2.22) of the atomic ground state. A heuristic scheme of accounting for the effects of a long-range part of the potential, notably for a Coulomb potential, on the dipole moment, has recently been formulated [22] on the basis of Eqs. (2.20)–(2.22). It has the most noticeable effect on the low-energy part of the harmonic spectrum around the binding energy.

Equation (2.15) suggests the following interpretation: the second term describes the atom interacting with the laser field (absorbing and emitting photons) up to the time t, at which it emits the harmonic photon and returns to the ground state. The third term is the complex conjugate of the second, where the events unfold in the opposite time order. Formally, the third term is required in order that $\mathbf{R}(t)$ be real. The fourth term represents a continuum-continuum interaction in the following sense: the atom interacts with the field, emits the harmonic photon, *and keeps interacting with the field* before it finally returns to the ground state.

As to the range of validity of these results, the main approximation of $U\to U^{(V)}$ becomes more and more questionable as the range of the binding potential expands. In general, the dipole moments (2.16) or (2.20) should provide

reliable approximations for intensities such that the ponderomotive potential is not much smaller than the binding energy. For intensities approaching the over-the-barrier regime, the approach should still be valid, but one may have to insert the field-dependent energy shift of the ground state by hand. Moreover, ionization can no longer be ignored. It can be incorporated as described elsewhere [8]. Complete dressing of the ground state abandons the relative simplicity of the approach. For the zero range potential and $U_p \sim |E_0|$, it has been shown [5] that this does not noticeably affect any of the harmonics above the third.

Below, we will compare the results based on Eq. (2.20) with those based on Eqs. (2.16) and (2.17), both for the case of the zero-range potential. Quantitatively, we will find that in many circumstances the effects due to the fourth term of Eq. (2.15) are small. On the other hand, the above derivation shows that it is crucial in obtaining the compact result (2.16) and, consequently, the essentially exact solution for the zero-range potential.

C. Formal comparison of the two models

In Eqs. (2.16) and (2.17), a general potential $V(\mathbf{r})$ can be retained. Not specifying the potential, we can bring expression (2.16), which contains all four terms of Eq. (2.15), to a form that is quite close to the dipole moment (2.20). To this end, we first notice that, owing to the existence of the two terms in Eq. (2.18), it is possible to write Eq. (2.16) in the form

$$\mathbf{R}^{(K)}(t) = \int_{-\infty}^{t} dt' dt'' \frac{t-t'}{t'-t''} \int d^3p e^{-i|E_0|(t'-t'')} \times \exp[-iS(\mathbf{p},t',t'')] \langle 0| \left(\mathbf{r} - \frac{e}{m} \int_{t'}^{t} d\tau \mathbf{A}(\tau) \right) V|\mathbf{p} - e\mathbf{A}(t')\rangle \langle \mathbf{p} - e\mathbf{A}(t'')|V|0\rangle + \text{c.c.}, \quad (2.23)$$

which explicitly displays its reality. Again, we have made use of the decomposition of the Volkov time-evolution operator in Eq. (2.16) in terms of Volkov wave functions. The new form (2.23) contains matrix elements of the binding potential V. With the help of the Schrödinger equation, we can rewrite them as

$$\langle \mathbf{p}|V|0\rangle = -\left(|E_0| + \frac{1}{2m}\mathbf{p}^2 \right) \langle \mathbf{p}|0\rangle, \quad (2.24)$$

$$\langle \mathbf{p}|\mathbf{r}V|0\rangle = -\left(|E_0| + \frac{1}{2m}\mathbf{p}^2 \right) \langle \mathbf{p}|\mathbf{r}|0\rangle + \frac{i}{m}\mathbf{p}\langle \mathbf{p}|0\rangle, \quad (2.25)$$

where $|\psi_0(t)\rangle = |0\rangle \exp(i|E_0|t)$. In comparison to the dipole moment (2.20) the dipole moment (2.23) which is based on the complete Keldysh result (2.16) contains an additional integration over time. This is the price to be paid for retaining the continuum-continuum interaction. The additional integration is related to the time at which emission of the harmonic takes place which is now at some time earlier than t, while in Eq. (2.20) it was at t. We will see below that this has a marked effect on the polarization properties of the emitted harmonics which originate from the vector character of the dipole moment. In form (2.20), the direction of the vector $\mathbf{R}^{(K)}(t)$ is solely determined by the dipole moment $\mathbf{d}[\mathbf{p} - e\mathbf{A}(t)]$ at the same time t. In contrast, the vector character of the Keldysh form $\mathbf{R}^{(K)}(t)$ [Eq. (2.23)] also depends on the history ($t' < t$).

D. S-matrix element for one-photon emission

A different starting point for the same goal is the S-matrix element for the emission of exactly one photon with frequency Ω and polarization $\boldsymbol{\epsilon}$ such that the atom winds up in the ground state after the field has been turned off in the distant future,

$$S_{\boldsymbol{\epsilon}}(\Omega) = \boldsymbol{\epsilon} \cdot \int dt\ e^{i\Omega t} \langle \Psi^{(+)}(t)|e\mathbf{r}|\Psi^{(-)}(t)\rangle. \quad (2.26)$$

The S-matrix element is the Fourier transform of the matrix element

$$\mathbf{R}_S(t) = \langle \Psi^{(+)}(t)|\mathbf{r}|\Psi^{(-)}(t)\rangle, \quad (2.27)$$

which is closely related, but not identical to the ground-state expectation value (2.13) of the dipole moment. The state

$$|\Psi^{(-)}(t)\rangle \equiv |\Psi(t)\rangle = \lim_{t' \to -\infty} U(t,t')|\psi_0(t')\rangle \quad (2.28)$$

reduces to the unperturbed ground state at early times, and is identical to the one used above. However, as required for an S-matrix element, the state

$$\langle \Psi^{(+)}(t)| = \lim_{t' \to \infty} \langle \psi_0(t')|U(t',t) \quad (2.29)$$

is defined such that it reduces to the ground state of the atom in the *distant future*, after the pulse has left the interaction region. For the matrix element $\mathbf{R}_S(t)$, the manipulations following Eq. (2.14) proceed analogously, and instead of Eq. (2.16) we now obtain

$$\mathbf{R}_S^{(K)}(t) = -\int_t^{\infty} dt' \int_{-\infty}^{t} dt'' \langle \psi_0(t')|VU^{(V)}(t',t)\mathbf{r} \times U^{(V)}(t,t'')V|\psi_0(t'')\rangle, \quad (2.30)$$

which differs from $\mathbf{R}^{(K)}(t)$ only by the range of the temporal integrations. Now, with the help of Eqs. (2.30), (2.17), and (2.18) the S-matrix element (2.26) of single-photon harmonic generation can be written as

$$S_{\boldsymbol{\epsilon}}(\Omega) = -\int_{-\infty}^{\infty} dt' \int_{-\infty}^{t'} dt'' \int d^3\mathbf{r}' d^3\mathbf{r}'' \psi_0(\mathbf{r}'t')^* V(\mathbf{r}') \times \boldsymbol{\epsilon} \cdot \left\{ \int_{t''}^{t'} dt\ e^{i\Omega t} \mathbf{r}_{\text{class}}(t;\mathbf{r}'t';\mathbf{r}''t'') \right\} \times U^{(V)}(\mathbf{r}'t',\mathbf{r}''t'')V(\mathbf{r}'')\psi_0(\mathbf{r}''t''). \quad (2.31)$$

This expression affords a very appealing intuitive interpretation very much in line with previous arguments [13,14], but obtained here in the context of a rigorous analytical calculation. It shows that the S-matrix element can be envisioned as the coherent superposition of contributions associated with

the classical orbits (2.18). These orbits describe an electron that starts at the time t'' from some position $\mathbf{r}''$ within the range of the binding potential $V(\mathbf{r})$ and, under the influence of the laser field, returns at the *later* time t' to the position $\mathbf{r}'$, again within the range of the potential. Each orbit has as its weight the Volkov time-evolution operator $U^{(V)}(t',t'')$. This interpretation does not apply to result (2.16) of using the ground-state expectation value $\mathbf{R}(t)$ [Eq. (2.13)], as the latter does not obey the time ordering $t'>t>t''$. For the δ-function potential (2.19), the spatial integrations in Eq. (2.31) can be carried out, and yield

$$S_{\boldsymbol{\epsilon}}(\Omega)=-\frac{2\pi e\kappa}{m^2}\int_{-\infty}^{\infty}dt'\int_{-\infty}^{t'}dt''e^{-i|E_0|(t'-t'')}\times\boldsymbol{\epsilon}\cdot\left\{\int_{t''}^{t'}dt\ e^{i\Omega t}\mathbf{r}_{\rm class}(t;0t';0t'')\right\}U^{(V)}(0t',0t''). \tag{2.32}$$

This expression recovers a result presented earlier [21].

The dipole moment expectation value is required as the source term for the integration of the Maxwell equations. However, if just the harmonic emission of a single atom is to be considered, then the S-matrix element is the quantity of choice. In the Appendix, we will further investigate the properties of the S matrix, and relate it to the dipole-dipole correlation function. The relation between ionization and harmonic generation which we will present in the next subsection holds only for the S-matrix element.

E. Exact relation between ionization and harmonic generation

The matrix element $\mathbf{R}_S(t)$ has another attractive formal property. It can be represented as the functional derivative with respect to the driving electric field $\mathbf{E}(t)$ of the ground-state persistence amplitude

$$Z=\langle 0|T\ \exp\left(-i\int_{-\infty}^{\infty}d\tau\ \mathcal{H}_I(\tau)\right)|0\rangle. \tag{2.33}$$

The square of Z is the probability that after the passage of the laser pulse the atom is still in its ground state, and nothing else has happened. In Eq. (2.33), this amplitude is written down in the interaction representation, so that

$$\mathcal{H}_I(t)=e^{iH_0t}[-e\mathbf{r}\cdot\mathbf{E}(t)]e^{-iH_0t}, \tag{2.34}$$

where $H_0=\hat{\mathbf{p}}^2/2m+V(\mathbf{r})$ is the unperturbed atomic Hamiltonian and $|0\rangle$ is the ground-state wave function $|\psi_0(t)\rangle$ of Eq. (2.2) in the interaction representation. T denotes the time-ordering operator. It is now easy to see that

$$e\mathbf{R}_S(t)=\langle 0|T\ \exp\left(-i\int_{t}^{\infty}d\tau\ \mathcal{H}_I(\tau)\right)e\ e^{iH_0t}\mathbf{r}e^{-iH_0t}\times T\ \exp\left(-i\int_{-\infty}^{t}d\tau\ \mathcal{H}_I(\tau)\right)|0\rangle=-i\frac{\delta}{\delta\mathbf{E}(t)}Z, \tag{2.35}$$

which is the statement made above. This is the most general formal relation between ionization and high-harmonic generation. Unfortunately, it is of limited practical use as the functional derivative requires knowledge of Z for *arbitrary* electric fields $\mathbf{E}(t)$. A power series expansion of the exponentials generates the perturbation expansion of $\mathbf{R}_S(t)$.

The corresponding expression for $\mathbf{R}(t)$ is

$$e\mathbf{R}(t)=\langle 0|\left[T\ \exp\left(-i\int_{-\infty}^{t}d\tau\ \mathcal{H}_I(\tau)\right)\right]^{\dagger}e\ e^{iH_0t}\mathbf{r}e^{-iH_0t}\times T\ \exp\left(-i\int_{-\infty}^{t}d\tau\ \mathcal{H}_I(\tau)\right)|0\rangle. \tag{2.36}$$

If there had been any doubts, a comparison of expressions (2.35) and (2.36) clearly shows that they are not equivalent. In the Appendix, we will present a rigorous discussion of the S matrix, and show that it lends itself to a more clearcut interpretation in terms of emission processes where the initial and final states are well defined, as opposed to the dipole expectation value. Numerically, the two expressions produce largely identical results for all harmonics higher than the third.

III. POLARIZATION PROPERTIES OF THE HARMONICS

For a linearly polarized driving field, the emitted harmonics are again linearly polarized in the same direction. If, however, the incident field has elliptical polarization, then *a priori* it is only known that the polarization of the harmonics will rotate in the same plane as the driving field. As soon as one goes beyond lowest-order perturbation theory, the ellipticity and the orientation of the axis of the polarization ellipse will, in general, differ from those of the incident field. Since these effects probe the vector character of harmonic generation, they might provide a more stringent test of any theory than just the harmonic intensities.

Only recently have the polarization properties of the individual high harmonics for incident elliptical polarization become the object of experimental efforts. Two groups published results within different regimes: Weihe and coworkers measured the offset angles of the polarization ellipse [23,24] and the ellipticities [24] of comparatively low harmonics (around the ionization energy, that is, at the beginning of the plateau) of a Ti-sapphire laser in argon and nitrogen. The Saclay group compared the harmonics in various rare gases within and near the end of the plateau for the same wavelength [9,25]. Weihe and co-workers found no significant effect of the gas density on their data. The Saclay group, on the other hand, was able to compare their measurements to theoretical results on the basis of Eq. (2.20), both with and without propagation. These theoretical simulations indicate that propagation considerably affects the observed polarization properties, smoothing out to a large extent the details of the single-atom behavior, and agreement with the experimental data was only good when propagation was included [25].

In what follows we will display and compare single-atom polarization properties calculated by means of the zero-range potential as well as the effective-dipole model, the latter employing the bound-state wave function of the zero-range potential, for the elliptically polarized driving field with vector potentials

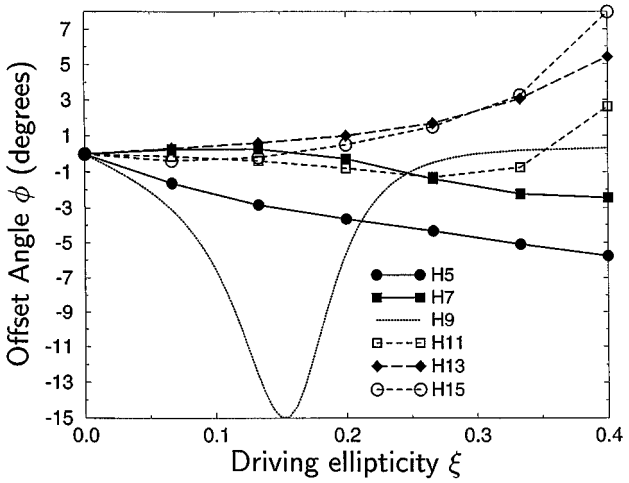

FIG. 1. Offset angle of the polarization ellipse of the 5th–15th harmonic vs the polarization ellipse of the driving field as a function of the ellipticity ξ of the driving field. The latter has a frequency of $\hbar\omega=1.578$ eV and an intensity of $I=5\times10^{14}$ W/cm^2 ($\eta=18.45$), and the atomic binding energy is $|E_0|/\hbar\omega=8.275$ corresponding to the first excited state of argon. These values are in close correspondence to the experiment of Ref. [23].

$$\mathbf{A}(t)=\left(\frac{4mU_p}{e^2(1+\xi^2)}\right)^{1/2}(\hat{\mathbf{x}}\cos\omega t+\xi\hat{\mathbf{y}}\sin\omega t), \qquad (3.1)$$

with ellipticity ξ and a ponderomotive energy U_p which is independent of the polarization. The dipole moments derived from either model contain all of the information necessary to extract offset angles, ellipticities, and whatever else one may be interested in.

A. Zero-range potential polarization properties

The calculations whose results we will show below are based on the S-matrix element (2.32). Explicit formulas giving the offset angle ϕ as well the harmonic ellipticity ξ' can be found in Ref. [26], along with some preliminary results.

First, we will show computations pertaining to the harmonics around the ionization energy. As a general feature, we find offset angles that vary quite erratically as a function of harmonic number, incident ellipticity, and intensity. Generally, the results have not too much in common with the data of Weihe and co-workers [23,24], which show offset angles rising linearly with increasing ellipticity of the driving field and harmonic ellipticities that generally exceed the driving ellipticity substantially. Weihe and co-workers made the observation that the offset angle tends to change sign when the harmonic energy goes through the ionization energy of the respective atom. In fact, we do find this behavior for appropriate parameters. Figure 1 exhibits such a case. The binding energy corresponds to the difference between the ground state and the first excited state of argon [27]; the wavelength is that of the experiments [23,24], and the intensity is quite high ($I=5\times10^{14}$ W/cm^2). However, we do not find this as a general feature. Figure 2 again shows a sequence of harmonics around the ionization energy for different parameters, and this time the sign of the offset angle oscillates from one harmonic to the next without any regular

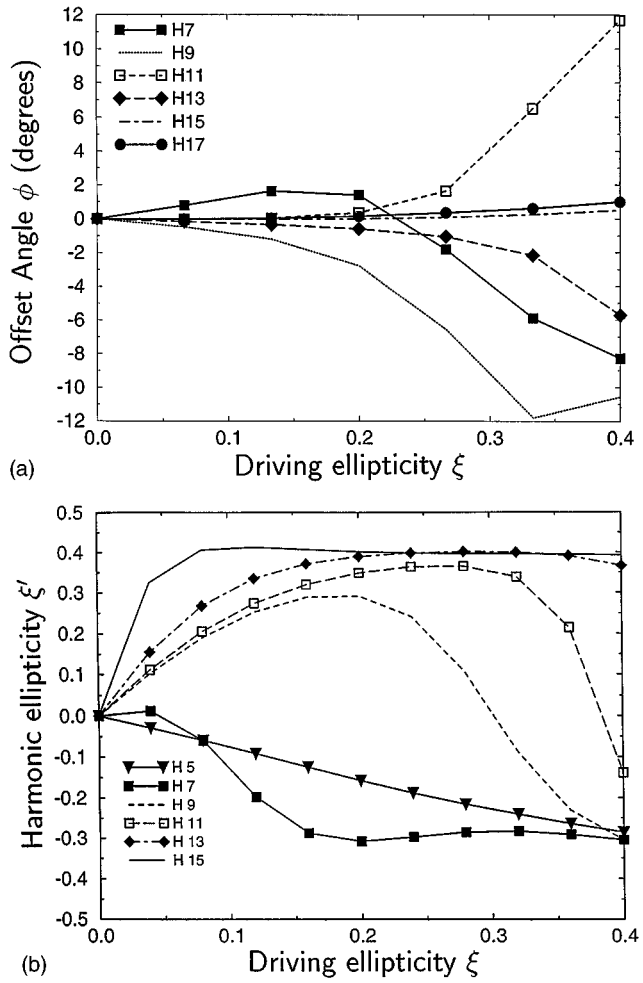

FIG. 2. Offset angles (a) and ellipticities (b) of the 7th–19th harmonic as a function of the ellipticity of the driving field for $\hbar\omega=1.17$ eV, $I=1.2\times10^{14}$ W/cm^2 ($\eta=10.58$), and $|E_0|/\hbar\omega=13.49$.

pattern. Figure 3 makes this behavior particularly evident. Here the offset angle for fixed driving ellipticity is plotted as a function of the driving intensity, which is expressed in terms of the dimensionless ratio of the ponderomotive potential over the energy of one laser quantum,

$$\eta=U_p/(\hbar\omega). \qquad (3.2)$$

The offset angle performs oscillations whose detailed shape is irregular, but which exhibit an approximate period of $\Delta\eta=1$. Most likely, this is related to the above-threshold ionization channel closings which occur at $\eta=\text{integer}-|E_0|/(\hbar\omega)$. It is known that these channel closings are reflected in pronounced sharp structures such as spikes in the harmonic intensities and phases [28]. In general, we notice that the zero-range potential produces harmonic offset angles that are smaller and less regular than those measured by Weihe and co-workers [23,24].

Second, in Figs. 4 and 5, we concentrate on the polarization properties of the harmonics around the rim of the plateau. Figure 4 displays the ellipticities and offset angles of the 53rd–63rd harmonic in a situation where the end of the plateau according to the classical model of Refs. [13,14] is at

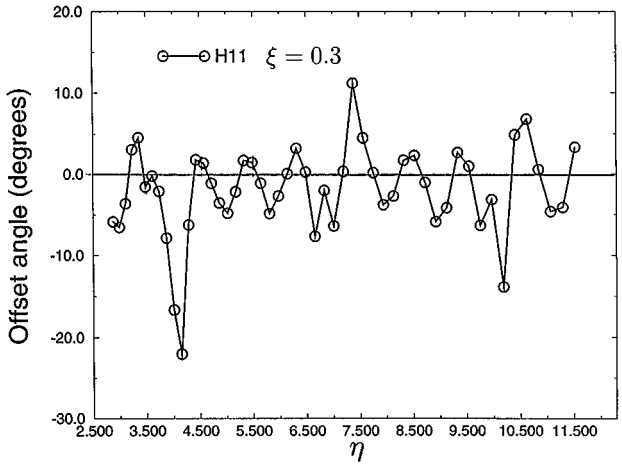

FIG. 3. Offset angle of the 11th harmonic as a function of the driving intensity expressed in terms of $\eta = U_p/\hbar\omega$ for an ellipticity of $\xi = 0.3$ of the driving field and $|E_0|/\hbar\omega = 13.49$. Very roughly, the offset angle changes sign with a period of $\Delta\eta = 1$.

$n_{\max} = |E_0| + 3.17\eta = 54.5$. The ellipticity of the 53rd harmonic still exhibits behavior characteristic of the plateau: as a function of the driving ellipticity, it fluctuates about zero with varying amplitudes. As for the 57th harmonic, the ellipticities increase monotonically with increasing driving ellipticity. The ellipticity of the 55th harmonic, which is closest to the classical $n_{\max}$, initially briefly changes sign before it follows the behavior of the 57th and all harmonics higher than that. The pattern of the corresponding offset angles is even more striking. With the harmonic number approaching $n_{\max}$, the offset angle rises more and more quickly. That is, already for smaller and smaller driving ellipticities does it rise to a large value not much below 90°. After the end of the plateau, it immediately settles to a value of near zero, where it stays henceforth for all of the harmonics higher than $n_{\max}$. This behavior is even more eye catching if we concentrate on a particular harmonic, and vary the driving intensity such that this harmonic slowly approaches the rim of the plateau before dropping over the edge. This is shown in Fig. 5. We see how the offset angle rears for a last time over a small interval of driving intensities, before it is almost instantly deflated.

B. Polarization properties in the effective-dipole model

In this section we shall compare the results based on the S-matrix element (2.32) with the results obtained from the effective-dipole model [Eq. (2.20)]. In order to evaluate the dipole moment from the latter formula, a fourfold integration, over the canonical momentum $\mathbf{p}$ and over t', has to be made. We performed this integration using a stationary phase approximation with respect to the relatively fast $\mathbf{p}$ dependence of the action $S(\mathbf{p},t,t')$. In order to make the comparison, we used the ground-state wave function $\psi_0(\mathbf{r})$ from the zero-range potential model. Explicit formulas giving the offset angle as well as the harmonic ellipticity can be found in Ref. [9]. A comparison of theory and experiment using this approach has yielded good agreement, and is discussed in Ref. [25]. It is worth emphasizing that the pulses employed in the experiment were as short as 25 fs.

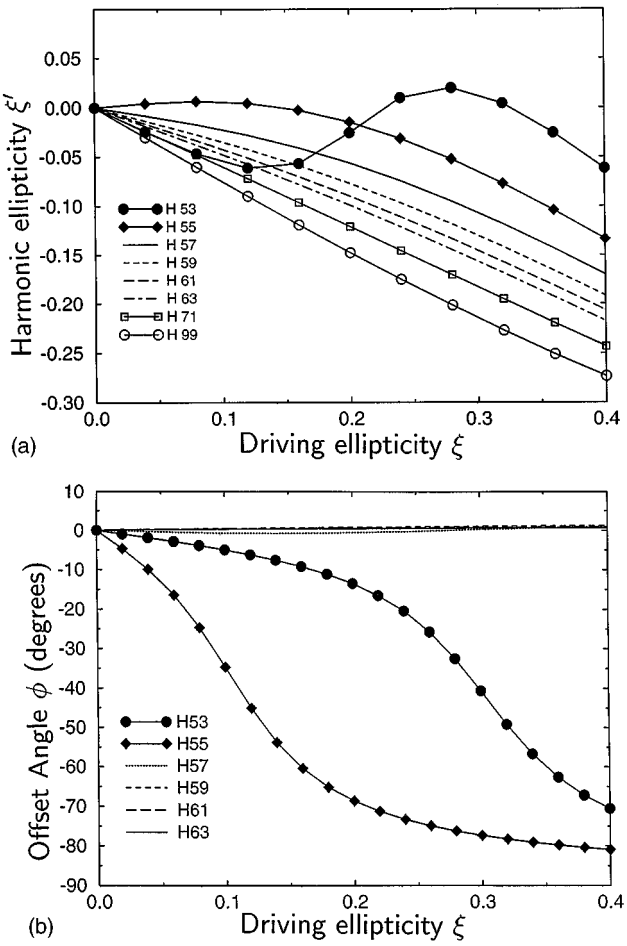

FIG. 4. Polarization properties of harmonics around the end of the plateau: (a) harmonic ellipticities, and (b) offset angle, both as a function of the ellipticity of the driving field. The parameters are $\hbar\omega = 1.17$ eV, $I = 1.2\times10^{14}$ W/cm^2 ($\eta = 10.58$), and $|E_0|/\hbar\omega = 20.93$. The formal cutoff is at $n_{\max} = |E_0|/\hbar\omega + 3.17U_p = 54.46$. Notice that for harmonics far beyond the end of the plateau (viz. H99) the harmonic ellipticities are consistently smaller than the driving ellipticity.

Here we show the computations pertaining to the harmonics around the rim of the plateau. In Fig. 6(a) we concentrate on the comparison of the ellipticities of the 53rd, 55th, and 57th harmonics in the same situation as in Fig. 4. The ellipticities calculated from the zero-range potential model (dashed lines) and effective-dipole model (solid lines) agree quite well. In the case of the offset angles [see Fig. 6(b)] the agreement is not as good, except for low ellipticities or in the cutoff region. In particular, the effective-dipole model does not predict the striking pattern of the corresponding offset angles obtained in Sec. III A for the harmonic number approaching $n_{\max}$. The offset angle predicted from the effective dipole model remains relatively small for the ellipticities considered. After the end of the plateau, both models are in agreement, and predict that the angle immediately settles to a value of near zero, where it stays henceforth for all of the harmonics higher than $n_{\max}$.

There are two possible reasons of these discrepancies: (a) expression (2.20) does not contain terms corresponding to the continuum-continuum interactions [the fourth term in Eq.

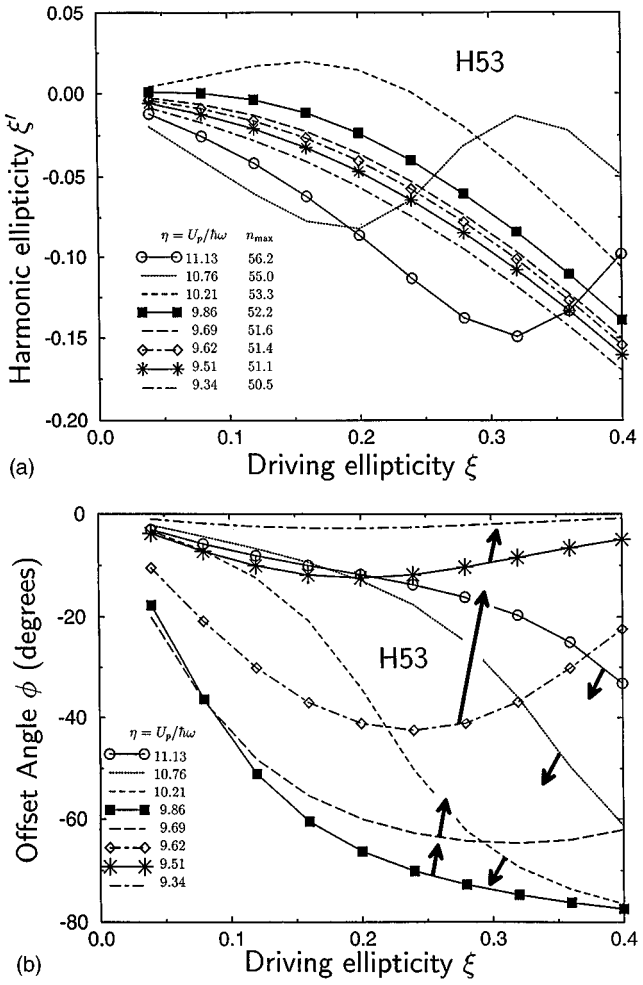

FIG. 5. Polarization properties of the 53rd harmonic for a range of intensities such that it is near the cutoff: (a) harmonic ellipticity, and (b) offset angle, both as a function of the driving ellipticity. The intensities are specified by the respective values of η. Otherwise, the parameters are those of Fig. 4. According to the $3.17U_p$ cutoff rule, the 53rd harmonic cuts off at $\eta = 10.12$. The curve for $\eta = 9.86$ approximately specifies the maximal offset angles reached. Intensities deviating by no more than 1.5% to either side of this value yield virtually identical offset angles. The arrows attached to the various curves in (b) point from one to the next in the order of decreasing driving intensity so that the 53rd harmonic is moving out of the plateau.

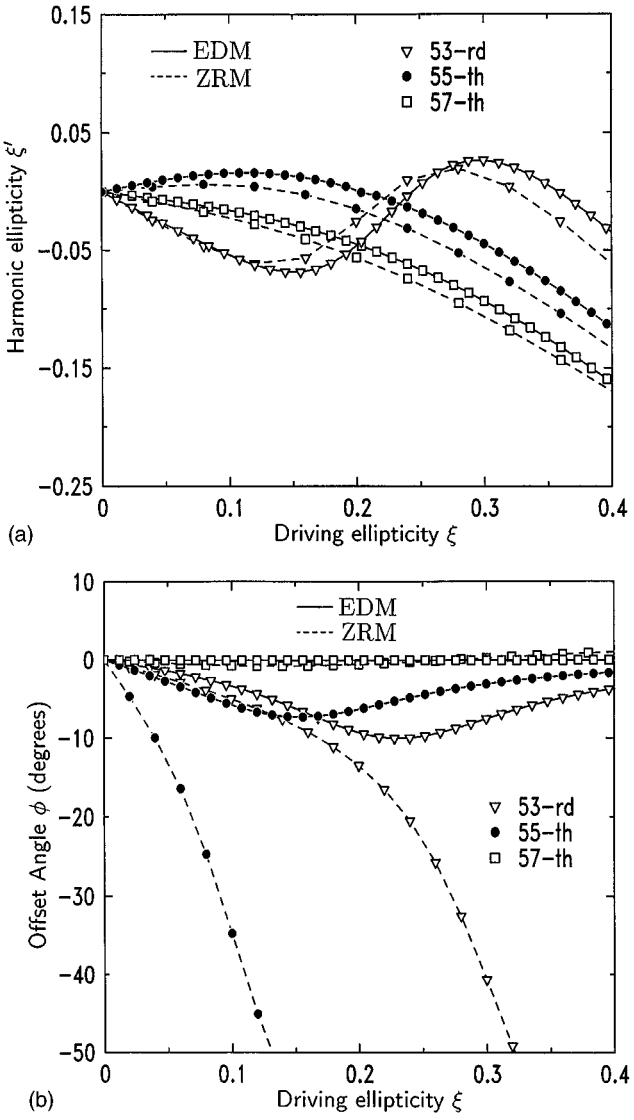

FIG. 6. Comparison of the polarization properties of harmonics near the end of the plateau calculated from the effective-dipole model [Eq. (2.20)] (EDM) using a zero-range potential wave function and the zero-range model [Eq. (2.32)] (ZRM), (a) harmonic ellipticities, and (b) offset angle. The parameters are the same as in Fig. 4, except that the intensity is smaller by 1%.

(2.15)]; (b) in the evaluation of Eq. (2.20) a stationary phase approximation was used to perform the integration with respect to **p**. Estimations of contribution (a), also based on the stationary phase approximation, suggest that most probably it is the latter approximation that causes the discrepancies. It should be stressed that, in the considered regime of parameters, both results depend rather dramatically on the driving intensity (see, for instance, Fig. 5). The error introduced by the stationary phase method may thus have significant consequences. On the other hand, the strong dependence on the driving intensity makes the effects predicted by the zero-range potential model difficult to observe in the macroscopic response of the atomic system in tight focusing conditions. That is probably the reason why the effective-dipole model [with approximations (a) and (b)] does reproduce the experimental data very well [25].

IV. CONCLUSIONS

In this paper we evaluated harmonic generation strictly parallel to the Keldysh-Faisal-Reiss (KFR) [15] framework for ionization. In particular, we derived general and explicit formulas for ionization amplitudes, dipole expectation values, and S-matrix elements for one photon emission valid for arbitrary atomic potentials. Generally, they are expected to apply under the same conditions as the KFR results for ionization, that is, in the strong-field limit. In the calculation of the ionization amplitudes, the KFR approach has to make one crucial approximation whose consequences are hard to estimate. This is the replacement of the final scattering state by a plane wave. For the calculation of harmonic generation, this approximation is not necessary, since the final atomic state is again the ground state. Therefore, one may expect that the KFR approach is more reliable for harmonic genera-

tion than for ionization. The requirement of a sufficiently high intensity becomes less stringent when the range of the binding potential shrinks. In particular, the zero-range potential results have been checked to be virtually exact for driving intensities up to $U_p \sim |E_0|$. For intensities approaching the over-the-barrier regime, the field-dependent shift of the ground-state energy as well as ionization must be and have been considered. The general expressions for the dipole moment can be applied to pulses of arbitrary length. Moreover, we discussed the relation between ionization and harmonic generation, and between the S-matrix element for one-photon emission and the dipole-dipole correlation function (see the Appendix).

Within our generalized theory we identified the expressions corresponding to the two models of harmonic generation discussed frequently in the literature: the zero-range potential model and the effective-dipole model. We discussed how both the aforementioned models fit in this more general context. We discussed and compared polarization properties of harmonics predicted by the two models. Both models agree quite well in many respects, but predict different results concerning the rotation angle of the polarization ellipse for the harmonics at the rim of the plateau. However, it is not yet clear whether or not the differences would still be noticeable after propagation through the medium.

ACKNOWLEDGMENTS

One of us (W. B.) would like to express his gratitude for the hospitality extended to him by the theory division of the Physik-Department of the Technical University of Munich. M. L. acknowledges fruitful discussions with Ph. Antoine, A. L'Huillier, and P. Salières. This work was supported in part by the Deutsche Forschungsgemeinschaft.

APPENDIX

In this appendix we will discuss the relation between the S-matrix element investigated in the main body of the paper and the dipole-dipole correlation function. It is well known that it is the latter that determines, in principle, the total number of harmonic photons emitted [29,30]. We employ a Hamiltonian where the incident laser field is treated classically, but for the time being we single out one particular mode for a quantized description. This is one of the modes into which spontaneous emission of a high harmonic will occur. Therefore we are able to define S-matrix elements for emission of a specified number of photons of this particular mode. Quantizing the entire harmonic spectrum would not introduce any additional problems, but just make the notation more clumsy.

Therefore, our Hamiltonian is

$$H = \Omega a^\dagger a + H_0 - e\mathbf{r}\cdot\mathbf{E}(t) - ieg\mathbf{r}\cdot\boldsymbol{\epsilon}(a - a^\dagger), \tag{A1}$$

where

$$H_0 = \frac{\hat{p}^2}{2m} + V, \tag{A2}$$

and $g = \sqrt{2\pi\Omega/V}$. In the interaction picture, we want to compute the S-matrix element for spontaneous emission of exactly one photon with polarization $\boldsymbol{\epsilon}$ and frequency Ω (that is, of the quantized mode) such that in the distant future the atom is again in its ground state $|g\rangle$ as it was in the remote past. It is

$$\begin{aligned} S_{\boldsymbol{\epsilon}}(\Omega) &= \langle \Omega\boldsymbol{\epsilon}, g \ \ \text{out}|0, g \ \ \text{in}\rangle = \langle \Omega\boldsymbol{\epsilon}, g|U_I(\infty, -\infty)|0, g\rangle \\ &= \langle 0, g|aU_I(\infty, -\infty)|0, g\rangle, \end{aligned} \tag{A3}$$

with

$$U_I(t, t') = T \ \exp\left(-i \int_{t'}^{t} d\tau \mathcal{H}_I(\tau) \right) \tag{A4}$$

and

$$\begin{aligned} \mathcal{H}_I(t) &= e^{i(H_0 + \Omega a^\dagger a)t} \left[-e\mathbf{r}\cdot\mathbf{E}(t) - e\mathbf{r}\cdot\boldsymbol{\epsilon} c\Omega(a + a^\dagger) \right] \\ &\quad \times e^{-i(H_0 + \Omega a^\dagger a)t} \\ &= -e\mathbf{r}(t)\cdot\left[\mathbf{E}(t) + ig\boldsymbol{\epsilon}(ae^{-i\Omega t} - a^\dagger e^{i\Omega t}) \right], \end{aligned} \tag{A5}$$

$$\mathbf{r}(t) = e^{iH_0 t}\mathbf{r}e^{-iH_0 t}. \tag{A6}$$

$\mathcal{H}_I(t)$ defined in Eq. (A5) differs from the one used in the main body of the paper, Eq. (2.34), by the quantization of the one particular mode. Commuting the annihilation operator in Eq. (A3) to the right, we can express the S-matrix element as the ground-state expectation value

$$S_{\boldsymbol{\epsilon}}(\Omega) = eg\boldsymbol{\epsilon}\cdot \int_{-\infty}^{\infty} dt \ e^{i\Omega t} \langle 0, g|U_I(\infty, t)\mathbf{r}(t)U_I(t, -\infty)|0, g\rangle. \tag{A7}$$

Next, we turn to the expectation number of the total number of spontaneously emitted photons, regardless of the final state of the atom. It is

$$N = \langle 0, g|U_I(\infty, -\infty)^\dagger a^\dagger a \ U_I(\infty, -\infty)|0, g\rangle \tag{A8}$$

$$\begin{aligned} &= \sum_i \sum_n \langle 0, g|U(\infty, -\infty)^\dagger a^\dagger|n\Omega\boldsymbol{\epsilon}, i\rangle \\ &\quad \times \langle n\Omega\boldsymbol{\epsilon}, i|aU(\infty, -\infty)|0, g\rangle. \end{aligned} \tag{A9}$$

The sum over intermediate states includes the entire spectrum $|i\rangle$ of the atom, and any number n of photons emitted. Owing to the action of the photon creation operators on the intermediate states, we can write the total photon number after the passage of the laser pulse in the form

$$N = \sum_i \sum_n n|\langle n\Omega\boldsymbol{\epsilon}, i \ \ \text{out}|0, g \ \ \text{in}\rangle|^2. \tag{A10}$$

In obvious notation, $\langle n\Omega\boldsymbol{\epsilon}, i \ \text{out}|0, g \ \text{in}\rangle$ refers to the S-matrix element for spontaneous emission of n photons with frequency Ω and polarization $\boldsymbol{\epsilon}$ such that the atom is in the ground state before the arrival of the laser pulse and in the state $|i\rangle$ after the pulse is gone. With high-harmonic emission the weak process that it is, the S-matrix elements $\langle \Omega\boldsymbol{\epsilon}, i|0, g\rangle$ for one-photon emission and, in particular, for the atom returning to the ground state ($i = g$) make the dominant contribution to the sum in Eq. (A10). To our knowl-

edge, harmonic emission, such that the atom winds up in some excited state, has never been observed experimentally, even though the process exists in principle, of course. It is the one-photon S-matrix element $\langle \Omega\boldsymbol{\epsilon},g \text{ out}|0,g \text{ in}\rangle$ that we investigated in the main body of this paper.

If, on the other hand, we commute the photon creation operators in Eq. (A8) so that they act on the vacuum of the quantized mode, we may represent the total photon number as

$$N=e^2g^2\int_{-\infty}^{\infty}dt\ dt'\ e^{-i\Omega(t-t')}\langle 0,g|\boldsymbol{\epsilon}\cdot\boldsymbol{\mathcal{R}}(t)_S^{\dagger}\times\boldsymbol{\epsilon}\cdot\boldsymbol{\mathcal{R}}_S(t')|0,g\rangle, \tag{A11}$$

where

$$\boldsymbol{\mathcal{R}}_S(t)=U_I(\infty,t)\mathbf{r}(t)U_I(t,-\infty) \tag{A12}$$

is a Heisenberg representation of the position operator. It can easily be checked that it satisfies a Heisenberg equation of motion corresponding to the Hamiltonian (A1). Hence the total photon number is related to the dipole-dipole correlation function (A11) for the Heisenberg position operator (A12), and, according to

$$\langle 0g|\boldsymbol{\mathcal{R}}_S(t)|0g\rangle=\mathbf{R}_S(t), \tag{A13}$$

the latter is essentially identical to the quantity $\mathbf{R}_S(t)$ [Eq. (2.27)], which the discussion of much of this paper was built upon.

On the other hand, the total photon number $N(t)$ at any time t can be represented as well in terms of the more commonly used dipole expectation value, as defined in Eq. (2.14),

$$\mathbf{R}(t)=\langle 0g|\boldsymbol{\mathcal{R}}(t)|0g\rangle, \tag{A14}$$

with

$$\boldsymbol{\mathcal{R}}(t)=\langle 0g|U_I(t,-\infty)^{\dagger}\mathbf{r}(t)U_I(t,-\infty)|0g\rangle, \tag{A15}$$

which is Hermitian. Then [29,30]

$$N(t)=e^2g^2\int_{-\infty}^{t}dt'\ dt''\ e^{-i\Omega(t'-t'')}\langle 0,g|\boldsymbol{\epsilon}\cdot\boldsymbol{\mathcal{R}}(t')\times\boldsymbol{\epsilon}\cdot\boldsymbol{\mathcal{R}}(t'')|0,g\rangle, \tag{A16}$$

and it is easy to show that $\lim_{t\to\infty}N(t)=N$. However, the decomposition (A10) of the total photon number in terms of the well-defined S-matrix elements of the individual channels only holds for representation (A11). Also, the intuitive interpretation of the harmonic-generation process expressed in Eq. (2.31) rigorously only holds for the S matrix. The significance of the ground-state expectation value (2.13) to the process of harmonic generation is that it is this quantity that enters the classical Maxwell equations as a source. It is not, however, in principle strictly related to the number of photons radiated by a single atom.

After the formal developments have been finished, the quantization of the one particular mode can be removed again. With the quantization left in place self-energy corrections due to this one particular quantized mode would result, which we may safely neglect in comparison to the much more important level shifts introduced by the external (nonquantized) laser field. Removing the quantization, we are left with

$$S_{\boldsymbol{\epsilon}}(\Omega)=eg\boldsymbol{\epsilon}\cdot\int_{-\infty}^{\infty}dt\ e^{i\Omega t}\langle g|U_{\mathrm{IE}}(\infty,t)\mathbf{r}(t)U_{\mathrm{IE}}(t,-\infty)|g\rangle, \tag{A17}$$

with

$$U_{\mathrm{IE}}(t,t')=T\ \exp\left(ie\int_{t'}^{t}d\tau\ \mathbf{r}(\tau)\cdot\mathbf{E}(\tau)\right). \tag{A18}$$

The vacuum expectation value of $U_{\mathrm{IE}}(t,t')$ in the limit where $t\to\infty$ and $t'\to-\infty$ yields the ground-state persistence amplitude Z, Eq. (2.33).

[1] A. L'Huillier, L.-A. Lompré, G. Mainfray, and C. Manus, in *Atoms in Intense Fields*, edited by M. Gavrila [Adv. At. Mol. Opt. Phys. Suppl. **1**, 139 (1992)].

[2] K. J. Schafer, J. L. Krause, and K. C. Kulander, Int. J. Nonlinear Opt. Phys. **1**, 245 (1992).

[3] K. C. Kulander, K. J. Schafer, and J. L. Krause, in *Atoms in Intense Fields* (Ref. [1]), p. 247.

[4] W. Becker, S. Long, and J. K. McIver, Phys. Rev. A **41**, 4112 (1990).

[5] W. Becker, S. Long, and J. K. McIver, Phys. Rev. A **50**, 1540 (1994).

[6] A. L'Huillier, M. Lewenstein, P. Salières, Ph. Balcou, M. Yu. Ivanov, J. Larsson, and C. G. Wahlström, Phys. Rev. A **48**, R3433 (1993).

[7] M. Lewenstein, Ph. Balcou, M. Yu. Ivanov, A. L'Huillier, and P. B. Corkum, Phys. Rev. A **49**, 2117 (1994).

[8] Both models can, in fact, account for both ground-state depletion and electron rescattering effects. See, Refs. [7,9] and [10], respectively, for the effective-dipole model, and Refs. [11] and [12] for the zero-range model.

[9] Ph. Antoine, A. L'Huillier, M. Lewenstein, P. Salières, and B. Carré, Phys. Rev. A **53**, 1725 (1996).

[10] M. Lewenstein, K. C. Kulander, K. J. Schafer, and P. Bucksbaum, Phys. Rev. A **51**, 1495 (1995).

[11] S. Long, Ph.D. dissertation, University of New Mexico, 1994.

[12] W. Becker, A. Lohr, and M. Kleber, J. Phys. B **27**, L325 (1994); **28**, 1931 (1995) (corrigendum).

[13] P. B. Corkum, Phys. Rev. Lett. **71**, 1994 (1993).

[14] K. C. Kulander, K. J. Schafer, and J. L. Krause, in *Super-Intense Laser-Atom Physics*, Vol. 316 of *NATO Advanced Study Institute, Series B: Physics*, edited by B. Piraux *et al.* (Plenum, New York, 1996), p. 95.

[15] L. V. Keldysh, Zh. Éksp. Teor. Fiz. **47**, 1945 (1964) [Sov. Phys. JETP **20**, 1307 (1965)]; F. H. M. Faisal, J. Phys. B **6**, L89 (1973); H. R. Reiss, Phys. Rev. A **22**, 1786 (1980).

[16] A. M. Perelomov, V. S. Popov, and M. V. Terent'ev, Zh. Éksp.

Teor. Fiz. **50**, 1393 (1966) [Sov. Phys. JETP Sov. Phys. JETP **24**, 207 (1967)].

[17] W. Becker, J. K. McIver, and M. Confer, Phys. Rev. A **40**, 6904 (1989).

[18] J. G. Cordes and M. G. Calkin, J. Phys. B **13**, 4111 (1980).

[19] M. V. Fedorov and J. Peatross, Phys. Rev. A **52**, 504 (1995).

[20] W. Becker, A. Lohr, and M. Kleber, Quantum Semiclass. Opt. **7**, 423 (1995).

[21] W. Becker, B. Gottlieb, A. Lohr, M. Kleber, G. G. Paulus, and H. Walther, in *Super-Intense Laser-Atom Physics IV*, Vol. 313 of *NATO Advanced Study Institute, Series 3: High Technology*, edited by H. G. Muller and M. V. Fedorov (Kluwer, Dordrecht, 1996), p. 109.

[22] M. Yu. Ivanov, Th. Brabec, and N. Burnett, Phys. Rev. A **54**, 742 (1996).

[23] F. A. Weihe, S. K. Dutta, G. Korn, D. Du, P. H. Bucksbaum, and P. L. Shkolnikov, Phys. Rev. A **51**, R3433 (1995).

[24] F. A. Weihe and P. H. Bucksbaum, J. Opt. Soc. Am. B **13**, 157 (1996).

[25] Ph. Antoine, B. Carré, A. L'Huillier, and M. Lewenstein, Phys. Rev. A **55**, 1314 (1997).

[26] A. Lohr, S. Long, W. Becker, and J. K. McIver, in *Super-Intense Laser-Atom Physics IV* (Ref. [21]), p. 477.

[27] It has been found before that agreement between the results of the zero-range potential and experimental data is often improved if the parameter $|E_0|$, originally the binding energy of the model atom, is adjusted to the energy difference between the ground state and the first excited state of the real atom, rather than just to its ground-state energy [5].

[28] W. Becker, S. Long, and J. K. McIver, Phys. Rev. A **46**, R5334 (1992).

[29] B. Sundaram and P. W. Milonni, Phys. Rev. A **41**, 6571 (1990).

[30] J. H. Eberly and M. V. Fedorov, Phys. Rev. A **45**, 4706 (1992).